HOKKAIDO UNIVERSITY

Title	BXSB/MpJ-Yaa mouse model of systemic autoimmune disease shows increased apoptotic germ cells in stage XII of the seminiferous epithelial cycle
Author(s)	Otani, Yuki; Ichii, Osamu; Masum, Abdul; Kimura, Junpei; Nakamura, Teppei; Elewa, Yaser Hosny Ali; Kon, Yasuhiro
Citation	Cell and tissue research, 381, 203-216 https://doi.org/10.1007/s00441-020-03190-0
Issue Date	2020-04-04
Doc URL	http://hdl.handle.net/2115/80847
Rights	This is a post-peer-review, pre-copyedit version of an article published in Cell and tissue research. The final authenticated version is available online at: http://doi.org/10.1007/s00441-020-03190-0
Type	article (author version)
File Information	Cell and tissue research_381_203-216.pdf

Instructions for use

Hokkaido University Collection of Scholarly and Academic Papers : HUSCAP

Title Page

BXSB/MpJ-*Yaa* mouse model of systemic autoimmune disease shows increased apoptotic germ cells in stage XII of the seminiferous epithelial cycle

Yuki Otani[1], Osamu Ichii[1,2], Md. Abdul Masum[1], Junpei Kimura[1], Teppei Nakamura[1, 3], Yaser Hosny Ali Elewa[1, 4], Yasuhiro Kon[1]*

1. Laboratory of Anatomy, Department of Basic Veterinary Sciences, Faculty of Veterinary Medicine, Hokkaido University, Kita 18 Nishi 9, Kita-ku, Sapporo, Japan
2. Laboratory of Agrobiomedical Regenerative Medicine, Faculty of Agriculture, Hokkaido University, Kita 9 Nishi 9, Kita-ku, Sapporo, Japan
3. Section of Biological Safety Research, Chitose Laboratory, Japan Food Research Laboratories, 2-3, Bunkyo, Chitose, Japan
4. Department of Histology, Faculty of Veterinary Medicine, Zagazig University, Zagazig, Egypt

*: Corresponding author (Tel: +81-11-706-5189; Email: y-kon@vetmed.hokudai.ac.jp).

Acknowledgments and Funding Information

This study was supported in part by JSPS KAKENHI (grant number JP18J22455). The research described in this paper was chosen for the Best Poster Presentation Award at the 6th Congress of Asian Association of Veterinary Anatomists in Malaysia (14-15 October 2017), and the Encouragement Award at the 161st Japanese Association of Veterinary Anatomists in Ibaraki (11-13 September 2018).

Abstract

In mammals, the reproductive system and autoimmunity regulate mutual functions. Importantly, systemic autoimmune diseases are thought to cause male infertility, but the underlying pathological mechanism remains unclear. In this study, the morpho-function of the testes in BXSB/MpJ-*Yaa* mice were analyzed as a representative mouse model for systemic autoimmune diseases to investigate the effect of excessive autoimmunity on spermatogenesis. At 12 and 24 weeks of age, BXSB/MpJ-*Yaa* mice showed splenomegaly and increased levels of serum autoantibodies, whereas no controls showed similar autoimmune condition. In histological analysis, the enlarged lumen of the seminiferous tubules accompanied with scarce spermatozoa in the epididymal ducts were observed in some of the BXSB/MpJ-*Yaa* and BXSB/MpJ mice, but not in C57BL/6N mice. Histoplanimetrical analysis revealed significantly increased residual bodies and apoptotic germ cells in the seminiferous tubules in BXSB/MpJ-*Yaa* testes without apparent inflammation. Notably, in stage XII of the seminiferous epithelial cycles, the apoptotic germ cell number was remarkably increased, showing a significant correlation with the indices of systemic autoimmune disease in BXSB/MpJ-*Yaa* mice. Furthermore, the Sertoli cell number was reduced at the early disease stage, which likely caused subsequent morphological changes in BXSB/MpJ-*Yaa* testes. Thus, our histological study revealed the altered morphologies of BXSB/MpJ-*Yaa* testes, which were not observed in controls, and statistical analysis suggested the effects of an autoimmune condition on this phenotype, particularly the apoptosis of meiotic germ cells. BXSB/MpJ-*Yaa* mice were shown to be an efficient model to study the relationship between systemic autoimmune disease and the local reproductive system.

Keywords: Systemic autoimmune disease; Male infertility; Spermatogenesis; Apoptosis; Meiosis

LIST OF ABBREVIATIONS

ASA: anti-sperm antibody

BTB: blood-testis barrier

BXSB: BXSB/MpJ-*Yaa*$^{+}$

BXSB-*Yaa*: BXSB/MpJ-*Yaa*

CB: citrate buffer

DNA: deoxyribonucleic acid

dsDNA: double-stranded DNA

EAO: experimental autoimmune orchitis

ELISA: enzyme-linked immunosorbent assay

Foxp3: forkhead box P3

IL: interleukin

lpr: lymphoproliferation

Nos: nitric oxide synthase

PAS: periodic acid-Schiff

RNA: ribonucleic acid

S/B: the ratio of spleen weight to body weight

SE: standard error

SLE: systemic lupus erythematosus

ssDNA: single-stranded DNA

St.: stage of seminiferous epithelial cycle

tACE: testicular isoform of angiotensin-converting enzyme

Tgf: transforming growth factor

Tlr: toll-like receptor

72 Tnf: tumor necrosis factor

73 Yaa: Y-linked autoimmune acceleration

1. Introduction

In mammals, immunity contributes to the maintenance of reproductive function. For female reproduction, the proper activation of local immunity by resident immune cells, such as macrophages and T-cells, plays a role in the ovulation or regression of the corpus luteum in the ovaries (Komatsu et al. 2003). In contrast, testes have a unique immunological feature, known as immune privilege. Immunosuppression is essential to maintain germ cells and appropriate spermatogenesis because components of germ cells that express after immune competence is established can be recognized as autoantigens and attacked by the immune system. Notably, the tight junction, called the blood-testis barrier (BTB) and formed by adjacent Sertoli cells, partially segregates spermatogenic cells from systemic immune factors and prevents systemic immune factors from invading the adluminal compartment. In addition, anti-inflammatory factors, such as Interleukin- (IL) 10 are produced by testicular interstitial cells and resident immune cells, to maintain an immunosuppressed environment (Fijak and Meinhardt 2006).

On the other hand, sex-related factors also affect the immune system. The X chromosome encodes several immune-associated genes, and several X-linked gene mutations have been determined as causing immunodeficiency. Briefly, a mutation in the γ-chain subunit forming IL-2, IL-4, IL-7, IL-9, IL-15, and IL-21 receptors causes X-linked severe combined immunodeficiency. Forkhead box P3 (*Foxp3*) is also identified as a causative gene for immune dysregulation, polyendocrinopathy, enteropathy, and X-linked syndrome in humans (Fish 2008). Furthermore, sex hormones play essential roles in the activation or suppression of the immune system. As a representative, estrogen receptors expressed in immune cells activate or suppress their functions, depending on the concentration of estrogen (Kovats 2015). Androgen appears to promote IL-10 secretion from T-cells and suppresses the function of dendritic cells or macrophages (Trigunaite et al. 2015).

Due to a close functional relationship between the immune and reproductive systems, abnormality in one system is often reflected in the other. In fact, 30% of patients with premature ovarian failure also have an autoimmune disease (Goswami and Conway 2007). Anti-sperm antibodies (ASA) are frequently detected in infertile men (Garcia et al. 2007), resulting in decreased sperm concentration and motility (Cui et al. 2015). Furthermore, secondary autoimmune orchitis leading to infertility is reported in patients with systemic autoimmune diseases, such as systemic lupus erythematosus (SLE), Behçet's disease, and rheumatoid arthritis. Furthermore, ASA is present in half of the patients with SLE (Silva et al. 2014). For research purposes, experimental autoimmune orchitis (EAO) can be induced by immunization with testicular homogenate and adjuvant in mice, rats, rabbits, and guinea pigs (Naito et al. 2012). EAO, resulting in infertility, is histopathologically characterized by T-cell-dependent lymphocytic inflammation and damaged seminiferous tubules, with disruption of the BTB (Kohno et al. 1983). In these patients and model animals, the abnormality of systemic or local immune systems causes reproductive system-related phenotypes, but detailed pathogenesis is unknown.

In this study, we examined the pathological features of the male reproductive system in a male-dominant systemic autoimmune disease mouse model. The BXSB strain is derived from an intercross of C57BL/6J and SB/Le mouse (Andrews et al. 1978). It has been found that some mutants in the BXSB strain are characterized by autoantibody production, splenomegaly, and severe lupus nephritis-like features due to the excessive proliferation of autoreactive lymphocytes (Suzuka et al. 1993). These mutants carry a Y-linked autoimmune acceleration (*Yaa*) mutation, a translocation of some genes on the X chromosome telomere region to that of the Y chromosome. *Yaa* mutation has been identified as the most potent causative molecule to mediate autoimmune disorder in these mutants, designated as BXSB/MpJ-*Yaa* (BXSB-*Yaa*,

122 Murphy and Roths 1979). In addition, previous studies revealed the BXSB genome is also
123 suspected of forming autoimmune disease-prone phenotypes, as aged female BXSB/MpJ
124 (BXSB, without *Yaa* mutation) mouse manifested autoantibody production and
125 glomerulonephritis (Boehm et al. 1998; Kimura et al. 2014).

126 Here we showed the histopathological abnormalities of the BXSB-*Yaa* testis, characterized
127 by increases of residual bodies and apoptotic germ cells in stage XII of the seminiferous
128 epithelial cycle, which were closely correlated with systemic autoimmune abnormalities. We
129 further demonstrated the change of Sertoli cell number was associated with the progression of
130 an autoimmune condition, which likely caused subsequent morphological changes in BXSB-*Yaa*
131 testes. Our results provide a novel insight into the pathogenesis of reproductive dysfunction
132 associated with systemic autoimmune abnormality.

2. Materials and methods

2.1. Animals and sample preparation

Male C57BL/6N, BXSB, and BXSB-*Yaa* mice were purchased from Japan SLC, Inc. (Hamamatsu, Shizuoka, Japan). Twelve- and 24-week-old mice were used in all experiments. Mice were maintained according to The Guide for the Care and Use of Laboratory Animals of Hokkaido University, and all animal experiments were approved by the Institutional Animal Care and Use Committee, Hokkaido University and the Faculty of Veterinary Medicine, Hokkaido University (approval No. 15-0079, 16-0124; approved by the Association for Assessment and Accreditation of Laboratory Animal Care International). Body weights were measured, followed by the collection of blood samples by cutting the carotid artery under deep anesthesia. After euthanasia by cervical dislocation, the testes, epididymides, and spleen were collected. The weights of the spleen and testes were measured, and the ratio to body weight was compared in each group, respectively.

2.2. Evaluation of serum autoantibodies

To evaluate the systemic autoimmune conditions, serum anti-double-stranded DNA (dsDNA) antibody levels were measured using the Mouse Anti-dsDNA ELISA KIT (Shibayagi, Gunma, Japan) according to the manufacturer's instructions.

2.3. Histological analysis

Collected organs were fixed in 4% paraformaldehyde (for immunohistochemistry) or Bouin's fluid overnight, were embedded in paraffin, then cut into sections (2-3 μm thick). Deparaffinized sections were stained with periodic acid-Schiff (PAS) to determine the stages of the seminiferous epithelial cycle (St.).

157 The immunodetection of cell markers for T-cells (CD3), B-cells (B220), macrophages (Iba1),
158 and apoptotic cells [single-stranded DNA (ssDNA)] was performed as follows: for antigen
159 retrieval, sections were incubated in buffered citrate (pH 6.0) for 15 min at 110°C. The samples
160 were soaked in methanol containing 0.3% H_2O_2 to block internal peroxidase activity. After
161 blocked in 10% normal goat serum (SABPO(R) Kit, Nichirei, Tokyo, Japan), or 10% normal
162 donkey serum (Sigma-Aldrich, Missouri, USA) for 1 hour at room temperature, sections were
163 incubated with primary antibodies listed in Table 1 at 4°C overnight. After washing 3 times in
164 Phosphate buffered saline, sections were incubated with biotin-conjugated goat anti-rabbit IgG
165 antibody (SABPO(R) Kit, Nichirei), or donkey anti-rat IgG antibody (Sant Cruz, California,
166 USA) for 30 min at room temperature, washed again, and incubated with streptavidin-biotin
167 complex (SABPO(R) Kit, Nichirei) for 30 min. The sections were then incubated with 3,
168 3'-diaminobenzidine tetrahydrochloride-H_2O_2 solution. Finally, the sections were counterstained
169 with PAS-hematoxylin staining. When the St. in more than 80% of the seminiferous tubules
170 could not be classified due to morphological abnormalities, these testis specimens were
171 excluded from the histoplanimetrical analysis.
172
173 ***2.4. Histoplanimetry***
174 Histoplanimetrical analysis for the testes was performed as follows:
175 (a) *The number and area of the seminiferous tubules*: Histological sections were converted
176 into digital images by scanning with NanoZoomer 2.0-RS and observed with
177 NDP.view2 program (Hamamatsu Photonics K.K., Hamamatsu, Shizuoka, Japan). In a
178 PAS-stained section, each St. of the seminiferous tubules was classified based on the
179 morphological characteristics of the seminiferous tubules (Meistrich and Hess 2013).
180 The number and area of the seminiferous tubules were quantified at each St. with

NDP.view2. These values were also used in the following measurements.

(b) *The number of residual bodies in seminiferous tubules*: Digitally imaged sections with NanoZoomer 2.0-RS were used. The numbers of residual bodies with more than 10 μm of the minor axis were counted at each classified St. according to analysis (a).

(c) *The number of ssDNA-positive cells in seminiferous tubules*: Sections digitally imaged with NanoZoomer 2.0-RS were used. The number of ssDNA-positive cells in a seminiferous tubule was counted at each classified St. according to analysis (a).

(d) *The number of Sertoli cells in seminiferous tubules*: Sections digitally imaged with NanoZoomer 2.0-RS were used. The number of Sertoli cells in a seminiferous tubule was counted at each classified St. according to analysis (a). The Sertoli cell was histologically identified by its basal localization and morphology with apparent nucleoli.

For quantification, the total numbers of residual bodies, ssDNA-positive cells, and Sertoli cells were divided by the total area of the seminiferous tubules at each St., in a section.

2.5. Reverse transcription and quantitative PCR (qPCR)

Total RNA was isolated from the testes using the TRIzol Reagent (Life Technologies, California, USA), following the manufacturer's protocol. cDNA was synthesized from total RNA by reverse transcription (RT) using the ReverTra Ace qPCR RT Master Mix with gDNA Remover (TOYOBO, Osaka, Japan). Gene expression levels were examined by using synthesized cDNA, THUNDERBIRD SYBR qPCR Mix (TOYOBO, Osaka, Japan), and a real-time thermal cycler (CFX Maestro; BIO-RAD, California, USA), according to the manufacturer's instructions. Gene expression in the testes was normalized to the expression of actin, beta (*Actb*). The details of primers are shown in Table 2.

205

206 ***2.6. Statistical analysis***

207 The results are expressed as mean ± standard error (SE) and were analyzed using
208 non-parametric statistical methods. Data among strains of the same age were compared using
209 the Kruskal-Wallis test, and multiple comparisons were performed using Scheffe's method when
210 significant differences were observed ($P < 0.05$). Data between different ages in the same strain
211 were compared using the Mann-Whitney *U*-test ($P < 0.05$). Spearman's correlation coefficient
212 ($P < 0.05$) was used to analyze the correlation between two parameters.

213 **3. Results**

214 ***3.1. Indices of the autoimmune condition and reproductive function of mice***

215 Figure 1a shows the bodyweight of animals. BXSB and BXSB-*Yaa* showed significantly
216 smaller values compared to C57BL/6N at 12 and 24 weeks of age, indicating early and late
217 disease stages, respectively. An age-related increase was observed in C57BL/6N and BXSB-*Yaa*,
218 but not in BXSB. The testis weight was compared as an index of male reproductive function
219 (Borg et al. 2010). At both ages, the testis weight was significantly smallest in BXSB-*Yaa*, and
220 BXSB also showed significantly lower values compared with C57BL/6N (Fig. 1b). No
221 significant age-related change was observed in their testis weights. For their ratio to body
222 weight, there was no significant strain difference at both ages, but age-related significant
223 decreases were observed in C57BL/6N and BXSB-*Yaa* (Fig. 1c).

224 The ratio of spleen weight to body weight (S/B) and serum anti-dsDNA antibody levels
225 were used as indices for the severity of systemic autoimmune disease in mice (Fig. 1d and e).
226 BXSB-*Yaa* showed significantly higher values of both indices compared with the other two
227 strains at both stages ($P < 0.01$). In these parameters, a significant age-related increase was
228 observed only in the S/B of BXSB-*Yaa*. Furthermore, the data of testis weight and spleen weight
229 in all examined BXSB-*Yaa* revealed a significant negative correlation ($\rho = -0.600$; $P = 0.001$, n
230 = 26) (Fig. 1f), indicating the close relationships between male reproductive function and
231 autoimmune disease.

232

233 ***3.2. Histopathological features of mouse testes***

234 Figure 2 shows representative histological images of mouse testes at 12 weeks of age.
235 Dilated seminiferous tubules with enlarged lumens were observed in some BXSB (12 and 24
236 weeks of age: 40%) and BXSB-*Yaa* (12 weeks of age: 67%; 24 weeks of age: 50%), but not in

C57BL/6N at both ages (Fig. 2a-c). As correlated with the enlargement of seminiferous tubules, the epididymal ducts at the tail portion in the C57BL/6N contained numerous spermatozoa, but not in some of the mice belonging to the other two strains at 12 weeks of age (Fig. 2d-f). These findings in the seminiferous tubules and the epididymal ducts were similarly observed at 24 weeks of age. Furthermore, multinucleated cells were observed in some seminiferous tubules of BXSB-*Yaa* testis (Fig. 2g), and some of their rete testis were dilated and filled with sperm at both ages (Fig. 2h). However, these features were not observed in C57BL/6N and BXSB at any age.

On the other hand, residual bodies, globular bodies comprising redundant organelles and RNA shed from elongating spermatid during spermiation (Firlit and Davis 1965), were observed in the seminiferous tubules of all mice at both ages (Fig. 2i-k). Some residual bodies were present in the seminiferous tubules throughout St. I to XII in BXSB-*Yaa* or at most stages except for St. II to V in BXSB, whereas they were mostly found at St. VIII or IX in C57BL/6N (Supplemental figure 1). The numerical analysis confirmed that BXSB-*Yaa* showed higher numbers of residual bodies in total tubular area compared to that of C57BL/6N at both ages, and the difference was significant at 12 weeks (Fig. 2l). In each stage comparison, significant differences among strains were observed only in St. VIII (Supplemental figure 1 and Fig. 2m). Briefly, BXSB-*Yaa* and BXSB tended to show a larger number than C57BL/6N at both ages, and a significant difference was observed between BXSB-*Yaa* and C57BL/6N. A significant age-related increase was observed only in C57BL/6N at St. VIII. Furthermore, some residual bodies with atypical morphologies, characterized by larger sizes and apoptotic like bodies (Creasy et al. 2012), were still stained with tACE, a specific marker of residual bodies, as a ring shape around the body (Supplemental Figure 2a) (Tung et al. 2017). These atypical structures were observed on the luminal side of the tubules at several St.s in BXSB-*Yaa* at both ages

(Supplemental Figure 2b and Fig. 2n) (Xiao et al. 2017). As atypical residual bodies produced during failure of spermiation due to chemical injection accumulate RNA (Saito et al. 2017), larger residual bodies observed in BXSB-*Yaa* seminiferous tubules contained abundant RNA stained with pyronin (Supplemental Figure 2c). The reaction of pyronin was confirmed to be eliminated with pre-treatment of RNase (Supplemental Figure 2d).

3.3. Comparison of immune-related phenotypes in mouse testes

Resident immune cells in testes and cytokines released from these cells or testicular cells are essential to maintain normal testicular function, such as the proliferation and apoptosis of germ cells, and establishment of BTB (Theas 2018). First, the infiltration and distribution of immune cells were analyzed by immunohistochemistry, since infiltrated immune cells as testicular inflammation affect spermatogenesis (Fig. 3). As a result, no CD3-positive T-cells and B220-positive B-cells were found in the testes of all examined strains at both ages (Fig. 3a-f). Iba1-positive macrophages were observed in the interstitium in all examined strains (Fig. 3g-i), but their distribution and appearance frequency did not alter among strains and ages (data not shown).

The mRNA expression levels of pro-/anti-inflammatory genes (*Il1a*, *Il1b*, *Nos2*, *Il6*, *Tnf*, *Tgf*, and *Il10*) in mice testes were evaluated by qPCR. There was no significant strain- or age-related difference among the examined strains (Fig. 3j).

3.4. Apoptotic cells in mouse testes

Apoptotic cell death is an essential process during spermatogenesis, in particular, for the removal of abnormal germ cells and maintaining the appropriate germ cell to Sertoli cell ratio (Giampietri et al. 2005). As a pathological condition, toxic, chemical, and genetic factors could

induce the apoptosis of germ cells (Shaha et al. 2010). Furthermore, in the testes with autoimmune orchitis, apoptotic germ cells are observed frequently, resulting in infertility (Naito et al. 2012). Immunohistochemical analysis was performed to detect apoptotic cells in the mouse testes, and Figure 4a to c show the representative images of ssDNA-positive apoptotic germ cells at 12 weeks, and they were observed in the seminiferous tubules of all strains at both ages. In numerical comparison, the mean number of ssDNA-positive germ cells in all examined areas of total tubules was highest in BXSB-*Yaa* compared with other strains at both ages (Fig. 4d). Notably, in the stage comparison, ssDNA-positive apoptotic germ cells were frequently observed in St. XII seminiferous tubules of all strains (Fig. 4e). Furthermore, significant differences among strains and ages were observed at St. XII as well as St. IV. For St. XII, BXSB-*Yaa* showed the highest values in both ages, and significances were observed with two other strains and C57BL/6N at 12 and 24 weeks of age, respectively. On the other hand, at 24 weeks, these positive cells in BXSB and BXSB-*Yaa* were significantly lower than in C57BL/6N at St. IV, and BXSB-*Yaa* showing the significant age-related decrease at this stage.

Next, the number of Sertoli cells in each stage of seminiferous tubules were evaluated to examine the effect of Sertoli cells on the number of apoptotic germ cells in the seminiferous tubules. The morphology of the Sertoli cells differed among St., and obvious strain- or age-related differences were not identified (Fig. 4f-h). In the numerical analysis, there was no strain- or significant age-related differences in the mean number of Sertoli cells in all examined areas of tubules, but BXSB-*Yaa* tended to show smaller values compared with C57BL/6N and BXSB at 12 weeks (Fig. 4i). Furthermore, at 12 weeks, BXSB-*Yaa* tended to show a smaller number of Sertoli cells at all St., and significances with BXSB were observed at St. IV, V, and IX (Fig. 4j). These decreased phenotypes of Sertoli cells were not observed in 24-week-old BXSB/MpJ-*Yaa* testes. An age-related increase was detected at St. IX in BXSB-*Yaa*.

3.5. Correlation between testicular phenotype and autoimmune disease indices in mice

Table 3 summarizes the statistical correlation between the examined indices for testicular phenotypes and autoimmune diseases in all examined mice or BXSB-*Yaa*. In all examined mice, the ratio of testis weight to body weight showed no significant correlation with other examined parameters. For histological phenotypes, the mean number of residual bodies in all examined areas of tubules positively correlated with the serum level of the dsDNA antibody in the groups, including 12 weeks and both ages. That of the ssDNA-positive cells in all examined areas of the tubules also positively correlated with S/B in all age groups and with the serum levels of the dsDNA antibody in the groups, including 24 weeks and both ages. In contrast, the number of Sertoli cells in all examined areas of the tubules negatively correlated with the serum levels of dsDNA antibody in the 12-week-old groups. In the analysis using BXSB-*Yaa*, testis weight to body weight significantly correlated with S/B in both age groups. The mean number of residual bodies in all examined areas of the tubules also positively correlated with S/B in the 12-week-old group. On the other hand, there was no correlation in the numbers of ssDNA-positive cells and Sertoli cells in all examined areas of the tubules.

Table 4 shows the statistical correlation of the indices of autoimmune diseases with histological phenotypes that showed significant differences in the strain comparison at each St. (Supplemental figure 1, Fig. 4e and j). In the analysis of all examined mice, the number of residual bodies in tubules at St. VIII positively correlated with the serum levels of the dsDNA antibody in the groups, including 12 weeks and both ages. As for the ssDNA-positive cells, there were positive correlations in St. XII tubules with S/B in the groups, including 24 weeks and both ages and with the serum levels of the dsDNA antibody in all age groups. That of the Sertoli cells in tubules at St. IV and V negatively correlated with S/B and the serum levels of the

dsDNA antibody in the 12-week groups. In tubules at St. IX, the Sertoli cell number positively correlated with S/B in the groups including both ages, but the coefficient was low. In the analysis using BXSB-*Yaa*, there was no definite correlation in residual bodies at St. VIII and Sertoli cells at St. IV and IX, although the number of Sertoli cells at St. V tubules positively correlated with S/B of 12 weeks. As for the number of ssDNA in tubules at St. IV, there was a positive correlation with S/B of 24 weeks. Furthermore, the number of positive cells in tubules at St. XII clearly showed a positive correlation with S/B and the serum levels of the dsDNA antibody in the 12-week-old groups. For other St. analysis, definite correlations were not shown (Supplemental Tables 1 and 2).

4. Discussion

BXSB-*Yaa* manifested the autoimmune disease phenotypes from 12 weeks, which became more severe at 24 weeks. The testis to body weight ratio decreased with disease progression and significantly correlated with the autoimmune index and spleen size in BXSB-*Yaa*. These data suggest that *Yaa* mutation-associated autoimmune abnormality can affect the male genital function. In general, the changes in testis weights reflect its histological changes, especially those of seminiferous tubules. Briefly, germ cell apoptosis inversely correlated with testis weight in mice (Otsuka et al. 2010). Indeed BXSB-*Yaa* increased the number of apoptotic germ cells. On the other hand, BXSB-*Yaa* and BXSB, but not C57BL/6N showed wider lumens of seminiferous tubules. This reasoning may be accurate as the increased luminal diameter of the seminiferous tubules was diagnosed as a dilation with increased fluid in the seminiferous tubules, which usually increases testis weight (Creasy et al. 2012). Since significant differences in the ratios of testis to body weight were not observed between healthy controls and BXSB-*Yaa*, the fluid accumulation in the testicular tubules could make testis weight loss obscure in BXSB-*Yaa*. Notably, nearly 95% of the seminiferous tubular fluid is reabsorbed in the efferent duct, and the failure of reabsorption causes fluid back pressure into seminiferous tubules, resulting in increased luminal diameter (Hess 2002). Further, the dysfunction of cilia in the efferent duct has been reported to cause male infertility with dilated seminiferous tubules and rete testis, which likely results from the failure to propel sperms from rete testis into the epididymis (Yuan et al. 2019; Terré et al. 2019). Importantly, inflammation could disrupt the morphology and function of ciliated epithelial cells (Ullrich et al. 2009; Thomas et al. 2010). Thus, the dilated seminiferous tubules would reflect the altered function of the efferent duct epithelium related to the fluid reabsorption or flow, and the inflammatory condition by the progression of systemic autoimmune disease in BXSB-*Yaa* might affect the epithelial cell

function.

In mammal testes, 75% of germ cells die during spermatogenesis through the process of apoptosis (Giampietri et al. 2005). In this study, BXSB-*Yaa* showed the increased apoptosis of St. XII at both disease stages but a decrease in that of St. IV with aging. In a previous study, we discussed that St. IV and St. XII were important for pachytene- or metaphase-specific germ cell apoptosis as checkpoints to maintain normal spermatogenesis, and the mouse genetic factors were found to affect their numbers (Otsuka et al. 2010). Therefore, the imbalanced checkpoint system between St. IV and St. XII might be involved in the quantitative alternations of apoptotic germ cells in BXSB-*Yaa*.

Importantly, St. XII showed the highest percentage among stages in the number of apoptotic germ cells of all examined mice. As for mouse St. XII, many germ cells undergo meiotic division. During meiosis, cells undergo complicated processes, such as chromosome replication, DNA double-strand break formation, spindle fiber formation, and meiotic cell division (Subramanian and Hochwagen 2014). Each process is regulated precisely and complexly; thus, some germ cells with errors undergo apoptosis at this stage (Lue et al. 2003). Notably, similar increases of dead cells at St. XII were reported in autoimmune disease-prone MRL/MpJ and MRL/MpJ-Fas$^{lpr/lpr}$ mice, but not in C57BL/10, CBA/J, C3H/He, BALB/c, DBA/2, NJL, and SL mice (Kon et al. 1999). Furthermore, our histoplanimetry revealed that the apoptotic cells at St. XII increased from the early disease stage and most strongly correlated with the autoimmune disease indices among examined parameters in BXSB-*Yaa*. Therefore, these results indicate that germ cells in St. XII tubules would have high susceptibility to altered immune conditions in mice and could be recognized as cells with errors.

BXSB-*Yaa* also showed the highest values in residual body numbers, in particular at St. VIII, among strains at both ages, and significantly correlated with the autoimmune disease index

390 at the early disease stage. A residual body is an aggregate of discarded organelles and RNA from
391 spermatogenic cells. Residual bodies are usually observed at St. VIII and IX, as they are
392 phagocytosed by Sertoli cells immediately after spermiation and then migrate to the basal
393 cytoplasm of Sertoli cells (Xiao et al. 2017). Furthermore, the abnormally large size of residual
394 bodies containing apoptotic like bodies and their appearance in St. where residual bodies are not
395 present normally, were sometimes observed in cases of spermiation failure, caused by chemical
396 injection (Creasy et al. 2012). Oral administration of one single chemical substance causes the
397 decrease of Sertoli cells and increase of residual bodies, which characterizes larger sizes and the
398 accumulation of RNA in rats (Saito et al. 2017). From these reports, it might be possible that the
399 change of testicular microenvironment caused by a systemic autoimmune condition in
400 BXSB-*Yaa* directly affects the process of spermiation. Further, as the number of residual bodies
401 at St. VIII tended to increase with aging in all examined mice, BXSB-*Yaa* would accelerate its
402 age-related functional loss of testicular cells.

403 The increased number of apoptosis of meiotic cells and abnormal residual bodies in
404 BXSB-*Yaa* strongly suggested impairment of Sertoli cell function because both structures are
405 usually phagocytized by Sertoli cells (Creasy et al. 2012; Jiang et al. 2015). Importantly, proper
406 clearance of apoptotic germ cells and residual bodies by Sertoli cells would be necessary to
407 prevent an autoimmune reaction against spermatogenic cells induced by autoantigens (Wu et al.
408 2008). Further, Sertoli cells are highly attributed toward maintaining the immune privilege of
409 mammalian testes, establishing BTB and immunosuppressive environments to segregate germ
410 cells from systemic autoimmunity (Fijak and Meinhardt 2006). Conversely, the current study
411 revealed that testicular antigens, which meiotic germ cells express, egress into interstitial space
412 through Sertoli cells, contributing toward maintaining immune tolerance (Tung et al. 2017).
413 Contradictory to immune privilege, systemic autoimmune diseases, such as SLE, Behçet's

414 disease, and rheumatoid arthritis, are diagnosed as associated diseases of autoimmune orchitis
415 leading to male infertility (Silva et al. 2014). Although the pathogenesis remains unclear, the
416 data for male patients with SLE suggest a dysfunction in Sertoli cells. (Suehiro et al. 2008).
417 Our histoplanimetric results revealed that Sertoli cells at St. IV-V and IX were significantly
418 decreased in BXSB-*Yaa* compared with BXSB at the early disease stage. Importantly, in
419 BXSB-*Yaa*, St. V and St. IX were the stages just after the spermatogenesis checkpoint at St. IV
420 and the frequent occurrence of residual bodies at St. VIII, respectively, suggesting the
421 relationship between Sertoli cells and germ cell alternations. On the other hand, a significant
422 decrease of apoptotic germ cells at St. IV was observed in BXSB-*Yaa* at the late but not the
423 early stage. In addition, these mice showed the age-related increase of Sertoli cells at St. IX.
424 Although the pathogenesis associating with Sertoli cells was still unclear in BXSB-*Yaa*, the
425 negative correlation between Sertoli cell numbers at St. IV-V and autoimmune disease severity
426 at the early stage indicated the effect of autoimmune abnormalities on Sertoli cells. Taken
427 together, further studies focusing on the direct effects of autoimmunity to germ cells as found in
428 increased apoptosis at St. XII and the indirect effects via Sertoli cell injuries at the other stages
429 would be beneficial.

430 From the genetic perspective, X-linked genes contribute to male reproductive function
431 including meiosis (Yang et al. 2008; Zheng et al. 2010). BXSB-*Yaa* possesses excessive
432 X-linked genetic factors, known as the genes on the *Yaa* locus (Murphy and Roths 1979), which
433 is considered to be responsible for systemic autoimmune disease. Among the genes on the *Yaa*
434 locus, Toll-like receptor 7 (*Tlr7*) and *Tlr8* are considered important for the development of
435 autoimmune disease condition (Pisitkun et al. 2006). Tlr is a pattern-recognition receptor
436 expressed on the cell or endosome membrane that plays a role in innate immunity. Notably, the
437 expression of *Tlr* members, including *Tlr7*, in mouse testis has been identified, and the roles of

438 the *Tlr* family in spermatogenesis have been discussed in a previous study (Wu et al. 2008).
439 Briefly, an *in vitro* study revealed that Tlr3 activation by polyinosinic-polycytidylic acid,
440 induced apoptosis of spermatogonia (Hu et al. 2015). In addition, a study using *Tlr*2- and
441 *Tlr4*-deficient mice showed that *Tlr2* and *Tlr4* contribute to the formation of autoimmune
442 orchitis (Liu et al. 2015). However, there has been no report on the involvement of *Tlr7* and
443 *Tlr8* in the male reproductive system. Therefore, these genes should be further examined as
444 candidate molecules that might be instrumental in connecting autoimmunity and the male
445 reproductive function.

446 In conclusion, our results highlight the effect of systemic autoimmune disease on
447 spermatogenesis, characterized with decreased testis weight, increased numbers of residual
448 bodies, and apoptotic germ cells, particularly in St. XII seminiferous tubules without typical
449 inflammation. In addition, we provide evidence for the possible effect of an autoimmunity
450 condition on Sertoli cells, which can subsequently cause the failure of spermatogenesis. Further
451 investigation of the mechanism of testicular phenotypes in BXSB-*Yaa* would reveal
452 pathogenesis of spermatogenesis disorder accompanying systemic autoimmune disease.

453

454

Compliance with Ethical Statements

Conflict of Interest

The authors have no conflicts of interest directly relevant to the content of this article.

Funding

This study was supported in part by JSPS KAKENHI (grant number JP18J22455) (Ms. Otani).

Ethical approval

All animal experiments were approved by the Institutional Animal Care and Use Committee, Hokkaido University and the Faculty of Veterinary Medicine, Hokkaido University (approval No. 15-0079, 16-0124; approved by the Association for Assessment and Accreditation of Laboratory Animal Care International).

References

Andrews BS, Eisenberg RA, Theofilopoulos AN, et al (1978) Spontaneous murine lupus-like syndromes. Clinical and immunopathological manifestations in several strains. J Exp Med 148:1198–215. doi: 10.1084/jem.148.5.1198

Boehm GW, Sherman GF, Hoplight BJ, et al (1998) Learning in Year-Old Female Autoimmune BXSB Mice. Physiol Behav 64:75–82. doi: 10.1016/S0031-9384(98)00027-4

Borg CL, Wolski KM, Gibbs GM, O'Bryan MK (2010) Phenotyping male infertility in the mouse: how to get the most out of a "non-performer". Hum Reprod Update 16:205–24. doi: 10.1093/humupd/dmp032

Creasy D, Bube A, de Rijk E, et al (2012) Proliferative and nonproliferative lesions of the rat and mouse male reproductive system. Toxicol. Pathol. 40

Cui D, Han G, Shang Y, et al (2015) Antisperm antibodies in infertile men and their effect on semen parameters: A systematic review and meta-analysis. Clin Chim Acta 444:29–36. doi: 10.1016/j.cca.2015.01.033

Fijak M, Meinhardt A (2006) The testis in immune privilege. Immunol Rev 213:66–81. doi: 10.1111/j.1600-065X.2006.00438.x

Firlit CF, Davis JR (1965) Morphogenesis of the residual body of the mouse testis. J Cell Sci s3-106: 93-98.

Fish EN (2008) The X-files in immunity: sex-based differences predispose immune responses. Nat Rev Immunol 8:737–744. doi: 10.1038/nri2394

Garcia PC, Rubio EM, Pereira OCM (2007) Antisperm antibodies in infertile men and their correlation with seminal parameters. Reprod Med Biol 6:33–38. doi: 10.1111/j.1447-0578.2007.00162.x

Giampietri C, Petrungaro S, Coluccia P, et al (2005) Germ cell apoptosis control during

493 spermatogenesis. Contraception 72:298–302. doi:
494 10.1016/J.CONTRACEPTION.2005.04.011
495 Goswami D, Conway GS (2007) Premature ovarian failure. Horm Res 68:196–202. doi:
496 10.1159/000102537
497 Hess RA (2002) The Efferent Ductules: Structure and Functions. In: The Epididymis: From
498 Molecules to Clinical Practice. Springer US, pp 49–80
499 Hu J, Song D, Luo G, et al (2015) Activation of Toll like receptor 3 induces spermatogonial
500 stem cell apoptosis. Cell Biochem Funct 33:415–422. doi: 10.1002/cbf.3133
501 Jiang X, Ma T, Zhang Y, et al (2015) Specific Deletion of Cdh2 in Sertoli Cells Leads to
502 Altered Meiotic Progression and Subfertility of Mice1. Biol Reprod 92:. doi:
503 10.1095/biolreprod.114.126334
504 Kimura J, Ichii O, Nakamura T, et al (2014) BXSB-type genome causes murine autoimmune
505 glomerulonephritis: Pathological correlation between telomeric region of chromosome 1
506 and Yaa. Genes Immun 15:182–189. doi: 10.1038/gene.2014.4
507 Kohno S, Munoz JA, Williams TM, et al (1983) Immunopathology of murine experimental
508 allergic orchitis. J Immunol 130:2675–82
509 Komatsu K, Manabe N, Kiso M, et al (2003) Changes in localization of immune cells and
510 cytokines in corpora lutea during luteolysis in murine ovaries. J Exp Zool 296A:152–159.
511 doi: 10.1002/jez.a.10246
512 Kon Y, Horikoshi H, Endoh D (1999) Metaphase-specific cell death in meiotic spermatocytes in
513 mice. Cell Tissue Res 296:359–369. doi: 10.1007/s004410051296
514 Kovats S (2015) Estrogen receptors regulate innate immune cells and signaling pathways. Cell
515 Immunol 294:63–69. doi: 10.1016/j.cellimm.2015.01.018
516 Liu Z, Zhao S, Chen Q, et al (2015) Roles of Toll-Like Receptors 2 and 4 in Mediating

517 Experimental Autoimmune Orchitis Induction in Mice1. Biol Reprod 92:. doi:
518 10.1095/biolreprod.114.123901
519 Lue Y, Sinha Hikim AP, Wang C, et al (2003) Functional Role of Inducible Nitric Oxide
520 Synthase in the Induction of Male Germ Cell Apoptosis, Regulation of Sperm Number,
521 and Determination of Testes Size: Evidence from Null Mutant Mice. Endocrinology
522 144:3092–3100. doi: 10.1210/en.2002-0142
523 Meistrich ML, Hess RA (2013) Assessment of spermatogenesis through staging of seminiferous
524 tubules. Methods Mol Biol 927:299–307. doi: 10.1007/978-1-62703-038-0_27
525 Murphy ED, Roths JB (1979) A y chromosome associated factor in strain bxsb producing
526 accelerated autoimmunity and lymphoproliferation. Arthritis Rheum 22:1188–1194. doi:
527 10.1002/art.1780221105
528 Naito M, Terayama H, Hirai S, et al (2012) Experimental autoimmune orchitis as a model of
529 immunological male infertility. Award Rev Med Mol Morphol 45:185–189. doi:
530 10.1007/s00795-012-0587-2
531 Otsuka S, Namiki Y, Ichii O, et al (2010) Analysis of factors decreasing testis weight in MRL
532 mice. Mamm Genome 21:153–161. doi: 10.1007/s00335-010-9251-0
533 Pisitkun P, Deane JA, Difilippantonio MJ, et al (2006) Autoreactive B cell responses to
534 RNA-related antigens due to TLR7 gene duplication. Science 312:1669–72. doi:
535 10.1126/science.1124978
536 Saito H, Hara K, Tanemura K (2017) Prenatal and postnatal exposure to low levels of
537 permethrin exerts reproductive effects in male mice. Reprod Toxicol 74:108–115. doi:
538 10.1016/J.REPROTOX.2017.08.022
539 Shaha C, Tripathi R, Mishra DP (2010) Male germ cell apoptosis: regulation and biology.
540 Philos Trans R Soc Lond B Biol Sci 365:1501–15. doi: 10.1098/rstb.2009.0124

541 Silva CA, Cocuzza M, Carvalho JF, Bonfá E (2014) Diagnosis and classification of
542 autoimmune orchitis. Autoimmun Rev 13:431–434. doi: 10.1016/J.AUTREV.2014.01.024
543 Subramanian V V, Hochwagen A (2014) The meiotic checkpoint network: step-by-step through
544 meiotic prophase. Cold Spring Harb Perspect Biol 6:a016675. doi:
545 10.1101/cshperspect.a016675
546 Suehiro RM, Borba EF, Bonfa E, et al (2008) Testicular Sertoli cell function in male systemic
547 lupus erythematosus. Rheumatology 47:1692–1697. doi: 10.1093/rheumatology/ken338
548 Suzuka H, Yoshifusa H, Nakamura Y, et al (1993) Morphological analysis of autoimmune
549 disease in MRL-lpr,Yaa male mice with rapidly progressive systemic lupus erythematosus.
550 Autoimmunity 14:275–82
551 Terré B, Lewis M, Gil-Gómez G, et al (2019) Defects in efferent duct multiciliogenesis underlie
552 male infertility in GEMC1-, MCIDAS- or CCNO-deficient mice. Dev 146:. doi:
553 10.1242/dev.162628
554 Theas MS (2018) Germ cell apoptosis and survival in testicular inflammation. Andrologia
555 50:e13083. doi: 10.1111/and.13083
556 Thomas B, Rutman A, Hirst RA, et al (2010) Ciliary dysfunction and ultrastructural
557 abnormalities are features of severe asthma. J Allergy Clin Immunol 126:. doi:
558 10.1016/j.jaci.2010.05.046
559 Trigunaite A, Dimo J, Jørgensen TN (2015) Suppressive effects of androgens on the immune
560 system. Cell Immunol 294:87–94. doi: 10.1016/j.cellimm.2015.02.004
561 Tung KSK, Harakal J, Qiao H, et al (2017) Egress of sperm autoantigen from seminiferous
562 tubules maintains systemic tolerance. J Clin Invest 127:1046–1060. doi:
563 10.1172/JCI89927
564 Ullrich S, Gustke H, Lamprecht P, et al (2009) Severe impaired respiratory ciliary function in

565 Wegener granulomatosis. Ann Rheum Dis 68:1067–1071. doi: 10.1136/ard.2008.096974
566 Wu H, Wang H, Xiong W, et al (2008) Expression Patterns and Functions of Toll-Like
567 Receptors in Mouse Sertoli Cells. Endocrinology 149:4402–4412. doi:
568 10.1210/en.2007-1776
569 Xiao C-Y, Wang Y-Q, Li J-H, et al (2017) Transformation, migration and outcome of residual
570 bodies in the seminiferous tubules of the rat testis. Andrologia 49:e12786. doi:
571 10.1111/and.12786
572 Yang F, Gell K, van der Heijden GW, et al (2008) Meiotic failure in male mice lacking an
573 X-linked factor. Genes Dev 22:682–91. doi: 10.1101/gad.1613608
574 Yuan S, Liu Y, Peng H, et al (2019) Motile cilia of the male reproductive system require
575 miR-34/miR-449 for development and function to generate luminal turbulence. Proc Natl
576 Acad Sci U S A 116:3584–3593. doi: 10.1073/pnas.1817018116
577 Zheng K, Yang F, Wang PJ (2010) Regulation of Male Fertility by X-Linked Genes. J Androl
578 31:79–85. doi: 10.2164/jandrol.109.008193
579
580
581

582

Table 1. Antibodies

Antibody	Source	Dilution	Antigen retrieval	Treatment
Rabbit anti-CD3	Nichirei (Tokyo, Japan)	1:200	10 mM CB (pH 6.0)	110°C, 15 min
Rat anti-B220	Cedarlane (Ontario, Canada)	1:1600	10 mM CB (pH 6.0)	110°C, 15 min
Rabbit anti-Iba1	Wako (Osaka, Japan)	1:1200	10 mM CB (pH 6.0)	110°C, 15 min
Rabbit anti-ssDNA	IBL (Gunma, Japan)	1:400	-	-

CB: citrate buffer. ssDNA: single-stranded DNA.

583

584

Table 2. Primers

Gene name (accession no.)	Official symbol	Primer sequence (5'-3')	Primer position (5'-3') (bp)	Product size (bp)
Actin, beta (NM_007393)	*Actb*	F: TGTTACCAACTGGGACGACA R: GGGGTGTTGAAGGTCTCAAA	334-353 498-479	165
Interleukin 1 alpha (NM_010554)	*Il1a*	F: AGATGACCTGCAGTCCATAACC R: GACAAACTTCTGCCTGACGAG	351-372 471-451	121
Nitric oxide synthase 2, inducible (NM_010927)	*Nos2*	F: AGCTGATGGTCAAGATCCAGAG R: GTGCATACCACTTCAACCCGA	1167-1188 1282-1262	116
Interleukin 1 beta (NM_008361)	*Il1b*	F: TTCCAGGATGAGGACATGAGC R: AATGGGAACGTCACACACCAG	337-357 447-427	111
Tumor necrosis factor (NM_013693)	*Tnf*	F: TCTTCTCATTCCTGCTTGTGGC R: CATAGAACTGATGAGAGGGAGGC	271-292 389-367	119
Interleukin 6 (NM_031168)	*Il6*	F: CAACGATGATGCACTTGCAGA R: GGTACTCCAGAAGACCAGAGGA	312-332 439-418	128
Interleukin 10 (NM_010548)	*Il10*	F: GCATTTGAATTCCCTGGGTGAG R: TTGTAGACACCTTGGTCTTGGAG	388-409 534-512	147
Transforming growth factor, beta 1 (NM_011577)	*Tgfb1*	F: ATGCTAAAGAGGTCACCCGC R: TGCTTCCCGAATGTCTGACG	1178-1197 1296-1277	119

585

586

587

Table 3. Correlation of autoimmune indices with examined parameters of the mouse testes

Parameter			T/B	Number of residual bodies in total	Number of ssDNA-positive cells in total	Number of Sertoli cells in total
			All / BXSB-*Yaa*	All / BXSB-*Yaa*	All / BXSB-*Yaa*	All / BXSB-*Yaa*
12-week-old	S/B	ρ	-.357 / -.400	.414 / .900*	.711** / -.700	-.443 / .500
		P	.191 / .505	.125 / .037	.003 / .188	.098 / .391
	Anti-dsDNA antibody	ρ	-.071 / .000	.767** / .800	.295 / -.600	-.600* / .300
		P	.800 / 1.000	.001 / .104	.286 / .285	.018 / .624
24-week-old	S/B	ρ	.111 / -.800	.489 / .100	.650** / -.500	.221 / .100
		P	.694 / .104	.064 / .873	.009 / .391	.428 / .873
	Anti-dsDNA antibody	ρ	.011 / -.500	.446 / -.200	.575* / .100	.321 / .700
		P	.970 / .391	.095 / .747	.025 / .873	.243 / .188
12- and 24-week-old	S/B	ρ	-.127 / -.758*	.296 / .200	.713** / -.539	-.057 / .552
		P	.504 / .011	.112 / .580	.000 / .108	.766 / .098
	Anti-dsDNA antibody	ρ	-.177 / -.345	.621** / .212	.400* / -.273	-.155 / .406
		P	.350 / .328	.000 / .556	.028 / .446	.414 / .244

*$P < 0.05$, ** $P < 0.01$. ρ: Spearman's rank correlation coefficient, N = 14-30 (all strains), 5-10 (BXSB-*Yaa*). All: C57BL/6N, BXSB, and BXSB-*Yaa*. T/B: ratio of testis weight to body weight; S/B: ratio of spleen weight to body weight; dsDNA: double-stranded DNA.

588 **Table 4. Correlation of autoimmune indices with examined parameters of the mouse testes**

Parameter			Number of residual bodies at St. VIII	Number of ssDNA-positive cells at St. IV	Number of ssDNA-positive cells at St. XII	Number of Sertoli cells at St. IV	Number of Sertoli cells at St. V	Number of Sertoli cells at St. IX
			All / BXSB-*Yaa*	All / BXSB-*Yaa*	All / BXSB-*Yaa*	All / BXSB-*Yaa*	All / BXSB-*Yaa*	All / BXSB-*Yaa*
12-week-old	S/B	ρ	.157 / -.300	.487 / .300	.470 / .900*	-.736** / .100	-.600* / .900*	.467 / .800
		P	.576 / .624	.065 / .624	.077 / .037	.002 / .873	.018 / .037	.079 / .104
	Anti-dsDNA antibody	ρ	.597* / -.100	.030/ .100	.567* / 1.000**	-.522* / .200	-.636* / .700	-.386 / .000
		P	.019 / .873	.914 / .873	.027 / .000	.046 / .747	.011 / .188	.155 / 1.000
24-week-old	S/B	ρ	.371 / .354	-.338 / .894*	.657** / -.100	.175 / .200	-.011 / -.100	.417 / -.300
		P	.173 / .559	.219 / .041	.008 / .873	.533 / .747	.970 / .873	.122 / .624
	Anti-dsDNA antibody	ρ	.482 / -.200	-.433 / -.112	.739** / .200	.236 / .200	.204 / .700	.411 / .000
		P	.069 / .747	.107 / .858	.002 / .747	.398 / .747	.467 / .188	.128 / 1.000
12- and 24-week-old	S/B	ρ	.290 / .406	.062 / -.485	.543** / .442	-.239 / .406	-.253 / .539	.392* / .333
		P	.121 / .244	.745 / .156	.002 / .200	.204 / .244	.178 / .108	.032 / .347
	Anti-dsDNA antibody	ρ	.567** / .042	-.249 / -.301	.624** / .527	-.174 / .333	-.255 / .564	.049 / .188
		P	.001 / .907	.185 / .339	.000 / .117	.359 / .347	.173 / .090	.795 / .603

*$P < 0.05$, ** $P < 0.01$. ρ: Spearman's rank correlation coefficient, N = 14-30 (all strains), 5-10 (BXSB-*Yaa*). All: C57BL/6N, BXSB, and BXSB-*Yaa*. T/B: ratio of testis weight to body weight; S/B: ratio of spleen weight to body weight; dsDNA: double-stranded DNA.

589 **Figure Legends**

590 **Figure 1. Indices of autoimmune disease condition and male reproductive function in mice**

591 (a) Bodyweight. (b) The ratio of spleen weight to body weight. (c) The concentration of
592 anti-dsDNA antibody in the serum. (d) Testis weight. (e) The ratio of testis weight to body
593 weight. Each bar represents mean ± SE ($n \geq 5$). Significant differences among strains are shown
594 by the letters above each bar. A lowercase letter represents the difference in 12-week-old mice.
595 An uppercase letter represents the difference in 24-week-old mice. $P < 0.05$ (Scheffe's method).
596 Significant differences between different ages in the same strain are indicated with an asterisk.
597 *: $P < 0.05$, **: $P < 0.01$ (Mann-Whitney *U*-test). (f) Correlation between the ratio of testis
598 weight to body weight and that of spleen in BXSB-*Yaa*. ρ: Spearman's rank correlation
599 coefficient ($n = 26$). $P = 0.001$.

600

601 **Figure 2. Comparison of histopathological features in mouse testes and epididymis**

602 (a-f) Representative images of the testes and epididymides of C57BL/6N (a and d), BXSB (b
603 and e), and BXSB-*Yaa* (c and f) at 12 weeks of age. Bidirectional arrows represent the lumen of
604 the seminiferous tubules. Asterisks (*) represent the loss of sperm in the lumen of the tail of the
605 epididymis. (g-h) Representative images of histopathology in BXSB-*Yaa* testis at 24 weeks (g)
606 and 12 weeks (h) of age. Arrowheads represent multinucleated cells. The asterisk shows the rete

607 testis dilated and filled with sperm. RT: rete testis. (i-k) Histology of St. VIII seminiferous
608 tubules of 12-week-old C57BL/6N (i), BXSB (j), and BXSB-*Yaa* (k). Arrowheads represent
609 residual bodies. (l-m) The number of residual bodies per unit area of total (l) and St. VIII
610 seminiferous tubules (m). Each bar represents mean ± SE (n = 5). Significant differences among
611 strains are shown by the letters above each bar. $P < 0.05$ (Scheffe's method). A lowercase letter
612 represents the difference in 12-week-old mice. An uppercase letter represents the difference in
613 24-week-old mice. Significant differences between different ages in the same strain are
614 indicated with an asterisk. *: $P < 0.05$ (Mann-Whitney *U*-test). (n) Representative image of an
615 atypical residual body in St. XII seminiferous tubules of 12-week-old BXSB-*Yaa*. All sections
616 were fixed with Bouin's fluid and stained with PAS-hematoxylin. Roman numerals indicate the
617 stage of the seminiferous epithelial cycle.
618
619 **Figure 3. Analysis of the immunological changes in mouse testes**
620 (a-i) Immunostained sections of mouse testes fixed with 4% paraformaldehyde.
621 Immunohistochemistry for CD3 (a-c), B220 (d-f), and Iba1 (g-i) in cross seminiferous tubules in
622 C57BL/6N, BXSB, and BXSB-*Yaa* at 12 weeks of age. Arrowheads represent macrophages.
623 Sections of the spleen are shown in insets. Bars = 100 μm. Bars (insets) = 10 μm.
624 (j) Relative mRNA expression of inflammation-related genes in C57BL/6N, BXSB, and

625 BXSB-*Yaa* testes. The expression levels were normalized to the levels of *Actb*. Each bar
626 represents mean ± SE (n = 5).
627
628 **Figure 4. Analysis of apoptotic cells in mouse testes**
629 (a-c) Immunostaining of ssDNA in cross seminiferous tubules at St. XII in 12-week-old
630 C57BL/6N (a), BXSB (b), and BXSB-*Yaa* (c). Arrowheads represent apoptotic cells. Bars = 50
631 μm.
632 (d-e) The number of ssDNA-positive cells per unit area of all examined (d) and each stage (e)
633 seminiferous tubules in a section of mouse testis. Each bar represents mean ± SE (n = 5).
634 Roman numerals indicate the stage of the seminiferous epithelial cycle. Significant differences
635 among strains are shown by the letters above each bar. $P < 0.05$ (Scheffe's method). A
636 lowercase letter represents the difference in 12-week-old mice. An uppercase letter represents
637 the difference in 24-week-old mice. Significant differences between different ages in the same
638 strain are indicated with an asterisk. *: $P < 0.05$, **: $P < 0.01$ (Mann-Whitney *U*-test).
639 (f-h) Histology of Sertoli cells in cross seminiferous tubules at St. IV-V in 12-week-old
640 C57BL/6N (f), BXSB (g), and BXSB-*Yaa* (h). Sections were fixed with Bouin's fluid and
641 stained with PAS-hematoxylin. Arrowheads represent Sertoli cells. Bars = 20 μm.
642 (i-j) The number of Sertoli cells per unit area of total (i) and each stage (j) seminiferous tubules

643 in a section of mouse testis. Each bar represents mean ± SE (n = 5). Roman numerals indicate
644 the stage of the seminiferous epithelial cycle. Significant differences among strains are indicated
645 with letters above each bar. $P < 0.05$ (Scheffe's method). A lowercase letter represents the
646 difference in 12-week-old mice. Significant differences between different ages in the same
647 strain are indicated with an asterisk. *: $P < 0.05$, **: $P < 0.01$ (Mann-Whitney *U*-test).
648

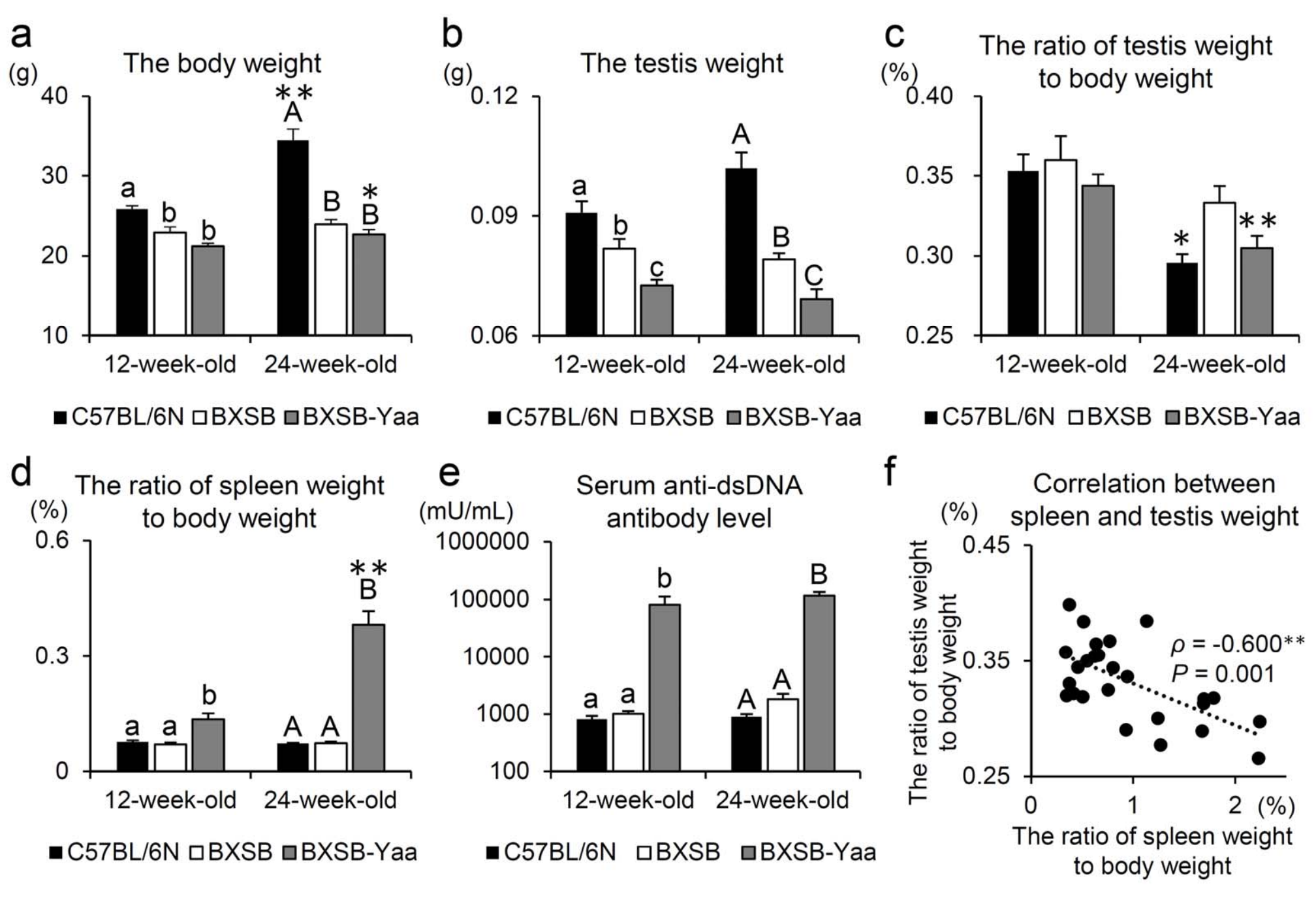
a
The body weight
(g)
40
30
20
10
a
b
b
A
B
B
**
*
12-week-old
24-week-old
C57BL/6N
BXSB
BXSB-Yaa
b
The testis weight
(g)
0.12
0.09
0.06
a
b
c
A
B
C
12-week-old
24-week-old
C57BL/6N
BXSB
BXSB-Yaa
c
The ratio of testis weight to body weight
(%)
0.40
0.35
0.30
0.25
*
**
12-week-old
24-week-old
C57BL/6N
BXSB
BXSB-Yaa
d
The ratio of spleen weight to body weight
(%)
0.6
0.3
0
a
a
b
A
A
B
**
12-week-old
24-week-old
C57BL/6N
BXSB
BXSB-Yaa
e
Serum anti-dsDNA antibody level
(mU/mL)
1000000
100000
10000
1000
100
a
a
b
A
A
B
12-week-old
24-week-old
C57BL/6N
BXSB
BXSB-Yaa
f
Correlation between spleen and testis weight
(%)
0.45
0.35
0.25
The ratio of testis weight to body weight
ρ = -0.600**
P = 0.001
0
1
2
(%)
The ratio of spleen weight to body weight

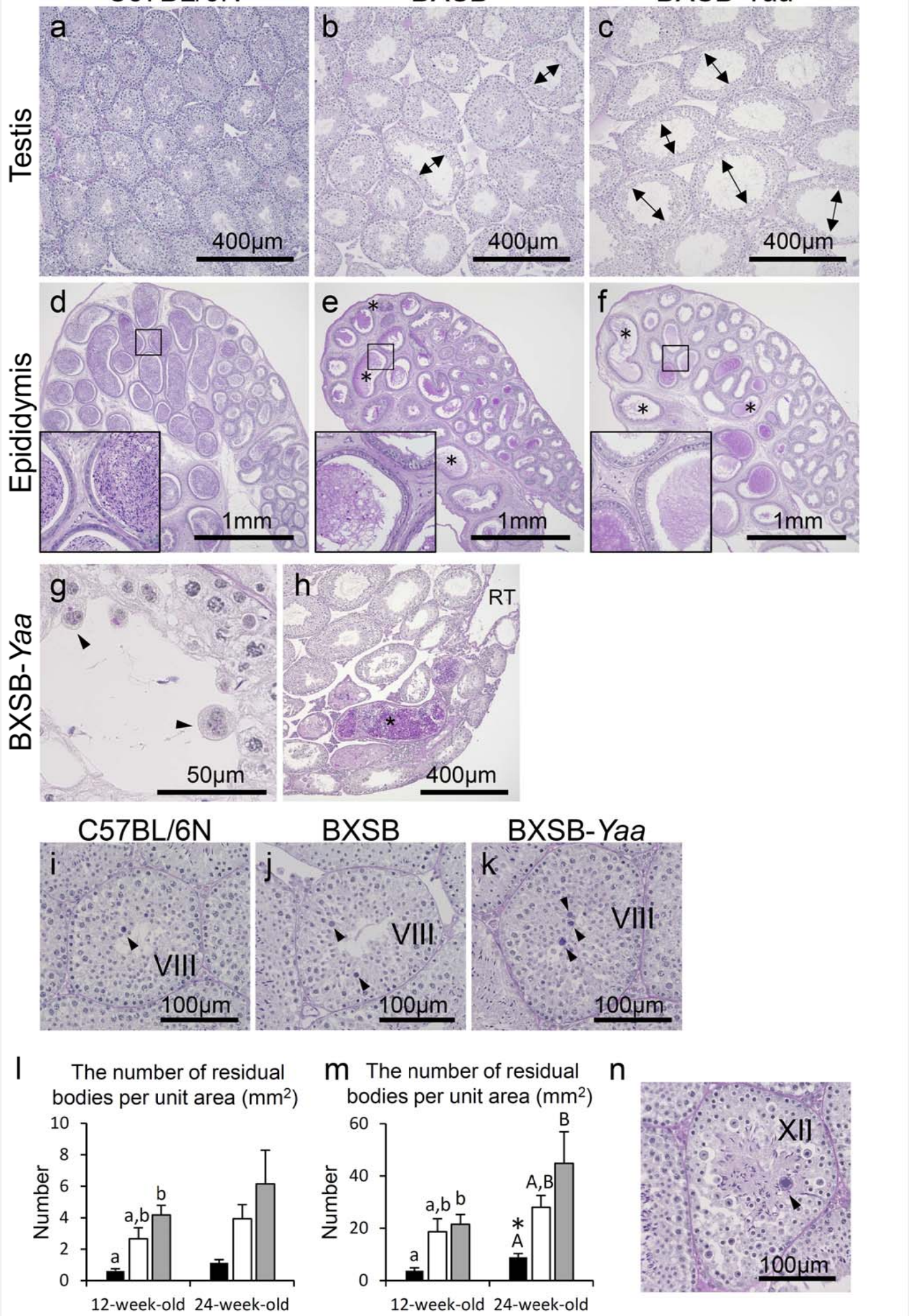
Testis
Epididymis
BXSB-Yaa
a
b
c
400μm
400μm
400μm
d
e
f
1mm
1mm
1mm
g
h
RT
50μm
400μm
C57BL/6N
BXSB
BXSB-Yaa
i
j
k
VIII
VIII
VIII
100μm
100μm
100μm
l
The number of residual bodies per unit area (mm2)
Number
12-week-old
24-week-old
m
The number of residual bodies per unit area (mm2)
Number
12-week-old
24-week-old
n
XII
100μm

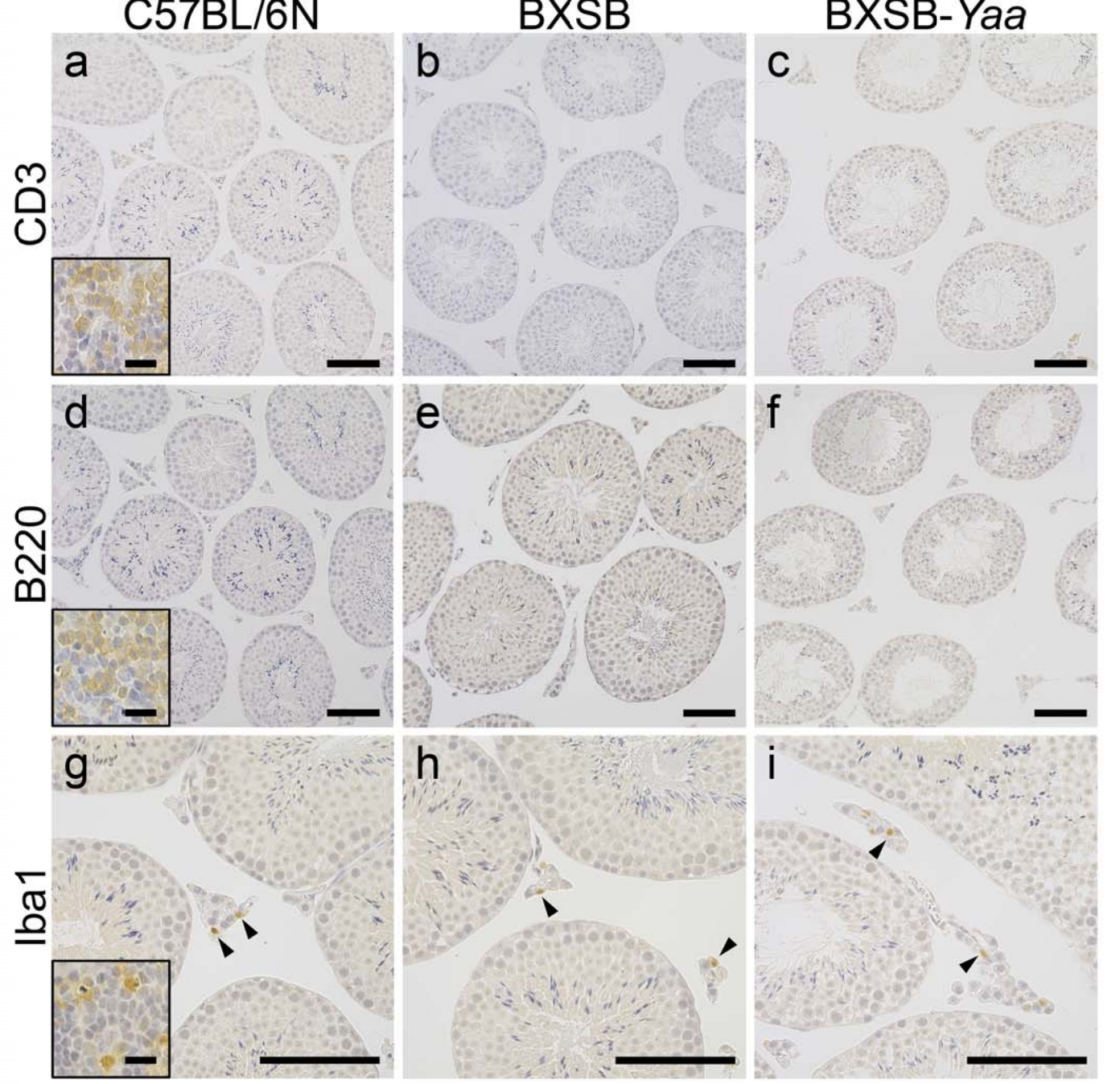
C57BL/6N
BXSB
BXSB-Yaa
CD3
B220
Iba1
a
b
c
d
e
f
g
h
i

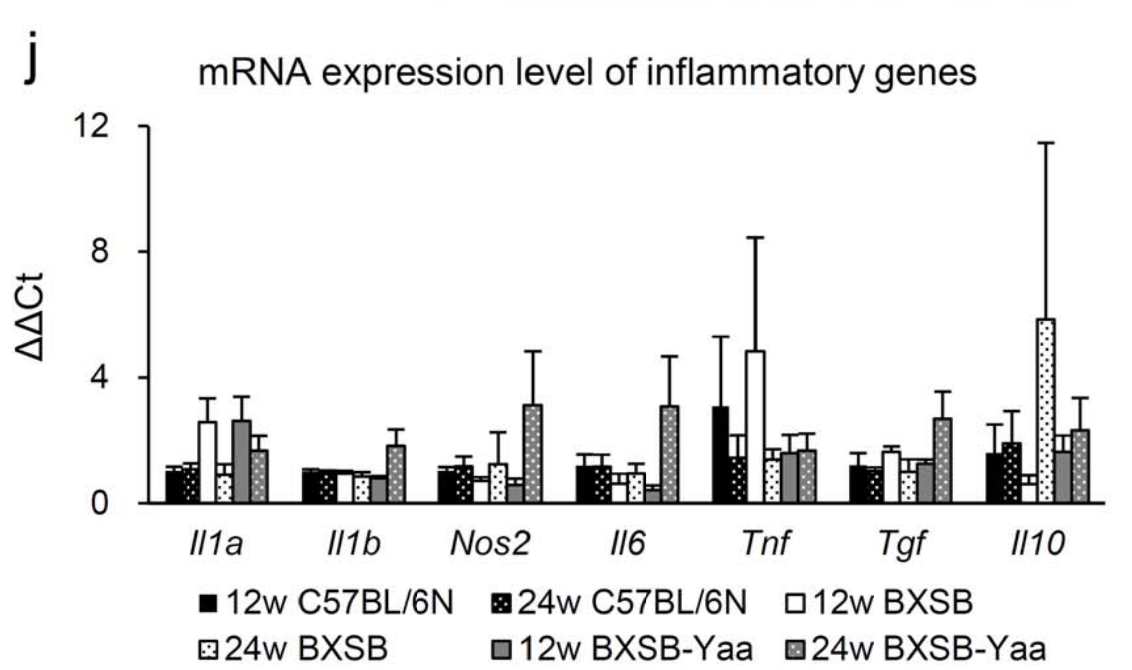
j
mRNA expression level of inflammatory genes
ΔΔCt
12
8
4
0
Il1a
Il1b
Nos2
Il6
Tnf
Tgf
Il10
12w C57BL/6N
24w C57BL/6N
12w BXSB
24w BXSB
12w BXSB-Yaa
24w BXSB-Yaa

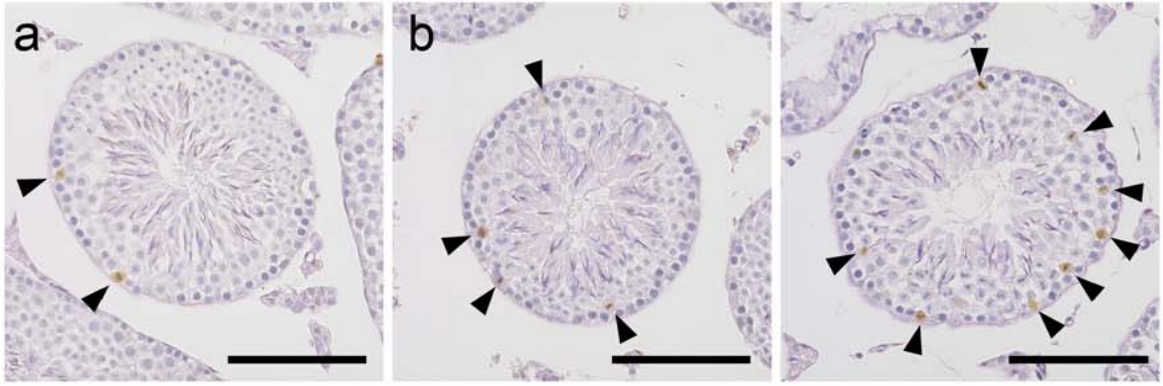
a
b

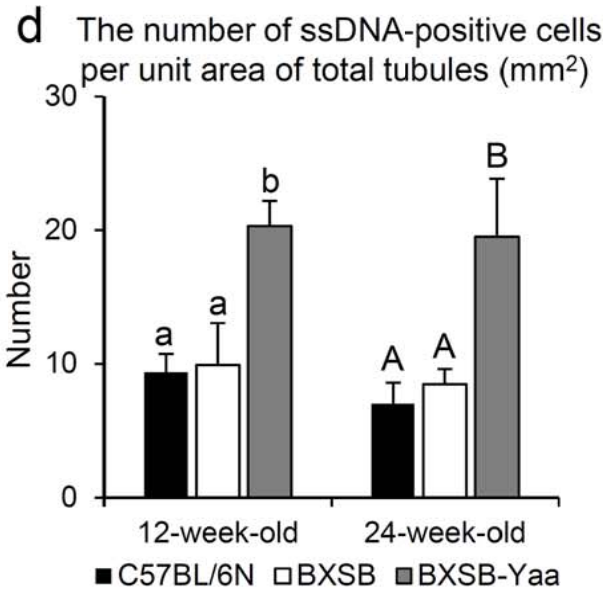
d
The number of ssDNA-positive cells per unit area of total tubules (mm2)
Number
30
20
10
0
a
a
b
A
A
B
12-week-old
24-week-old
C57BL/6N
BXSB
BXSB-Yaa

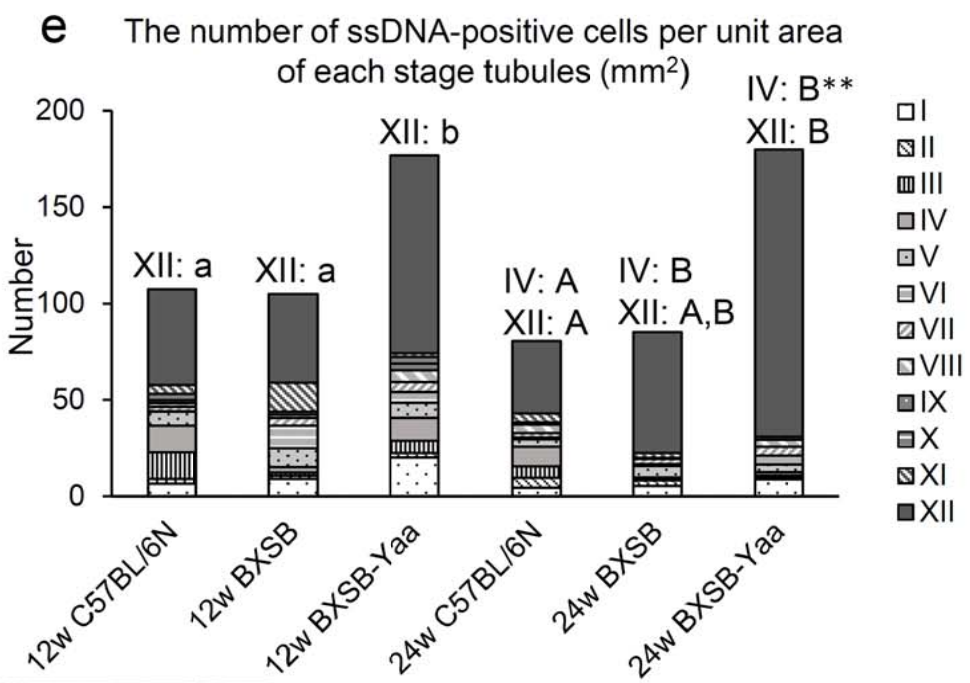
e
The number of ssDNA-positive cells per unit area of each stage tubules (mm2)
Number
200
150
100
50
0
XII: a
XII: a
XII: b
IV: A
XII: A
IV: B
XII: A,B
IV: B**
XII: B
12w C57BL/6N
12w BXSB
12w BXSB-Yaa
24w C57BL/6N
24w BXSB
24w BXSB-Yaa
I
II
III
IV
V
VI
VII
VIII
IX
X
XI
XII

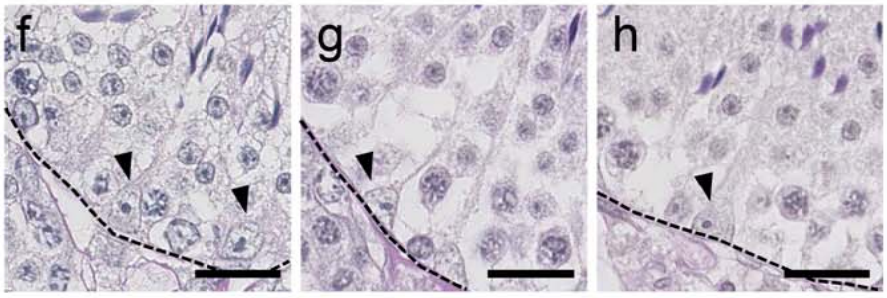
f
g
h

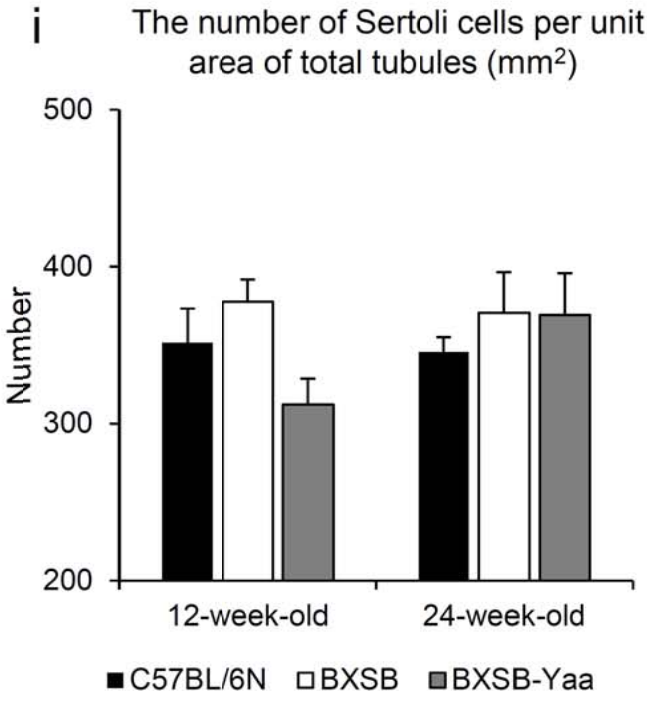
i
The number of Sertoli cells per unit area of total tubules (mm2)
Number
500
400
300
200
12-week-old
24-week-old
C57BL/6N
BXSB
BXSB-Yaa

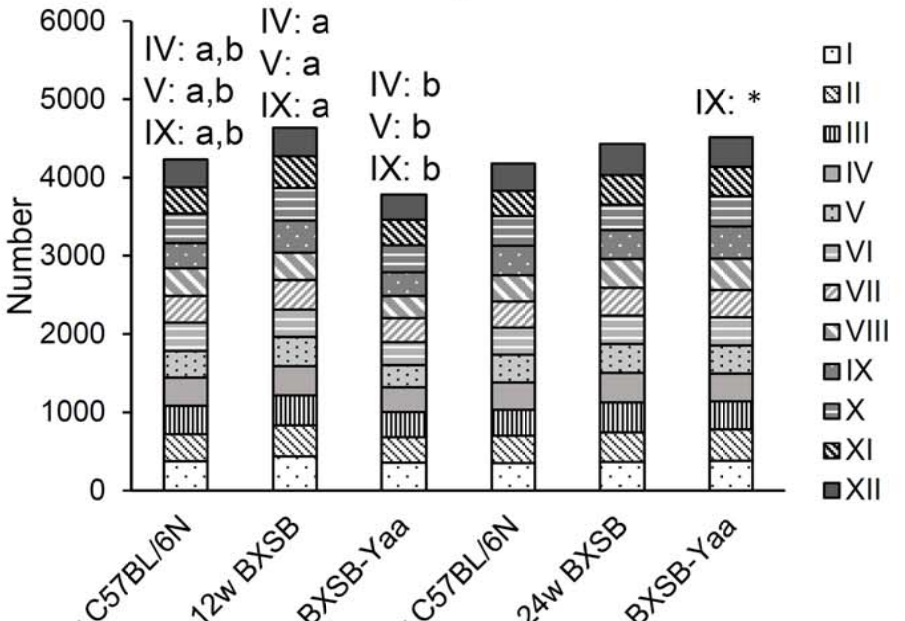
j
The number of Sertoli cells per unit area of each stage tubules (mm2)
Number
6000
5000
4000
3000
2000
1000
0
IV: a,b
V: a,b
IX: a,b
IV: a
V: a
IX: a
IV: b
V: b
IX: b
IX: *
12w BXSB
24w BXSB
I
II
III
IV
V
VI
VII
VIII
IX
X
XI
XII

Supplemental Table 1. Correlation of autoimmune indices with examined parameters in all mice

Parameter			Number of residual bodies	Number of ssDNA-positive cells	Number of Sertoli cells
12-week-old	S/B	ρ	-	I 0.624*; VIII 0.640*	IV -0.757**; V -0.600*
	Anti-dsDNA antibody	ρ	VIII 0.597*; IX 0.625*	XII 0.567*	IV -0.522*; V -0.636*; VI; -0.665**; VIII -0.617*
24-week-old	S/B	ρ	III 0.592*; VIII 0.579*	VI 0.524*; X -0.608*; XII 0.650**	-
	Anti-dsDNA antibody	ρ	-	XI -0.603*, XII 0.739**	-
12- and 24-week-old	S/B	ρ	III 0.433*; IX 0.392*	I 0.387*; VI 0.454*; XI -0.370*; XII0.543**	-
	Anti-dsDNA antibody	ρ	VIII 0.567**; IX 0.563**; X 0.430*	XI -0.417*, XII 0.624**	-

*P < 0.05, ** P < 0.01. ρ: Spearman's rank correlation coefficient, N = 15-30. All: C57BL/6N, BXSB, and BXSB-*Yaa.* S/B: ratio of spleen weight to body weight; dsDNA: double-stranded DNA.

Supplemental Table 2. Correlation of autoimmune indices with examined parameters in BXSB-*Yaa* mice

Parameter			Number of residual bodies	Number of ssDNA-positive cells	Number of Sertoli cells
12-week-old	S/B	ρ	VI 0.900*; VII 0.975**	XI 0.895*; XII 0.900*	V 0.900*
	Anti-dsDNA antibody	ρ	IX 0.900*	XII 1.000**	-
24-week-old	S/B	ρ	-	-	-
	Anti-dsDNA antibody	ρ	-	VI 0.900*	-
12- and 24-week-old	S/B	ρ	III 0.701*	III -0.725*	VIII 0.661*
	Anti-dsDNA antibody	ρ	-	-	VII 0.697*

*$P < 0.05$, ** $P < 0.01$. ρ: Spearman's rank correlation coefficient, N = 5-10 (BXSB-*Yaa*). S/B: ratio of spleen weight to body weight; dsDNA: double-stranded DNA.

Supplemental Figure 1

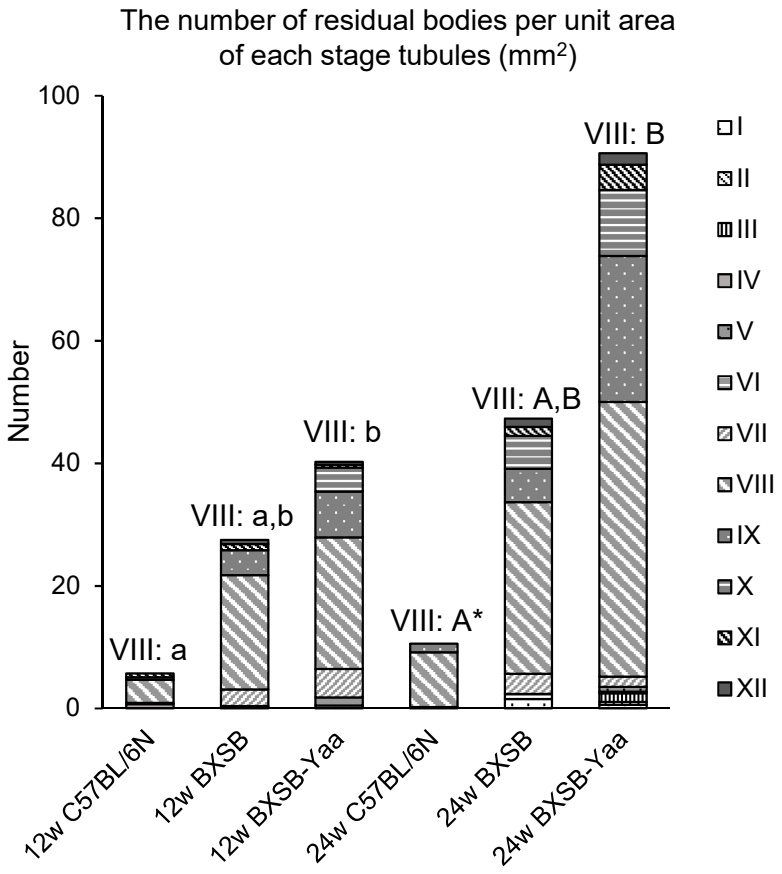

Supplemental Figure 1. The number of residual bodies per unit area of each St. seminiferous tubules. Each bar represents mean ± SE (n = 5). Significant differences among strains are shown by the letters above each bar. $P < 0.05$ (Scheffe's method). A lowercase letter represents the difference in 12-week-old mice. An uppercase letter represents the difference in 24-week-old mice. Significant differences between different ages in the same strain are indicated with an asterisk. *: $P < 0.05$ (Mann-Whitney *U*-test).

Supplemental Figure 2

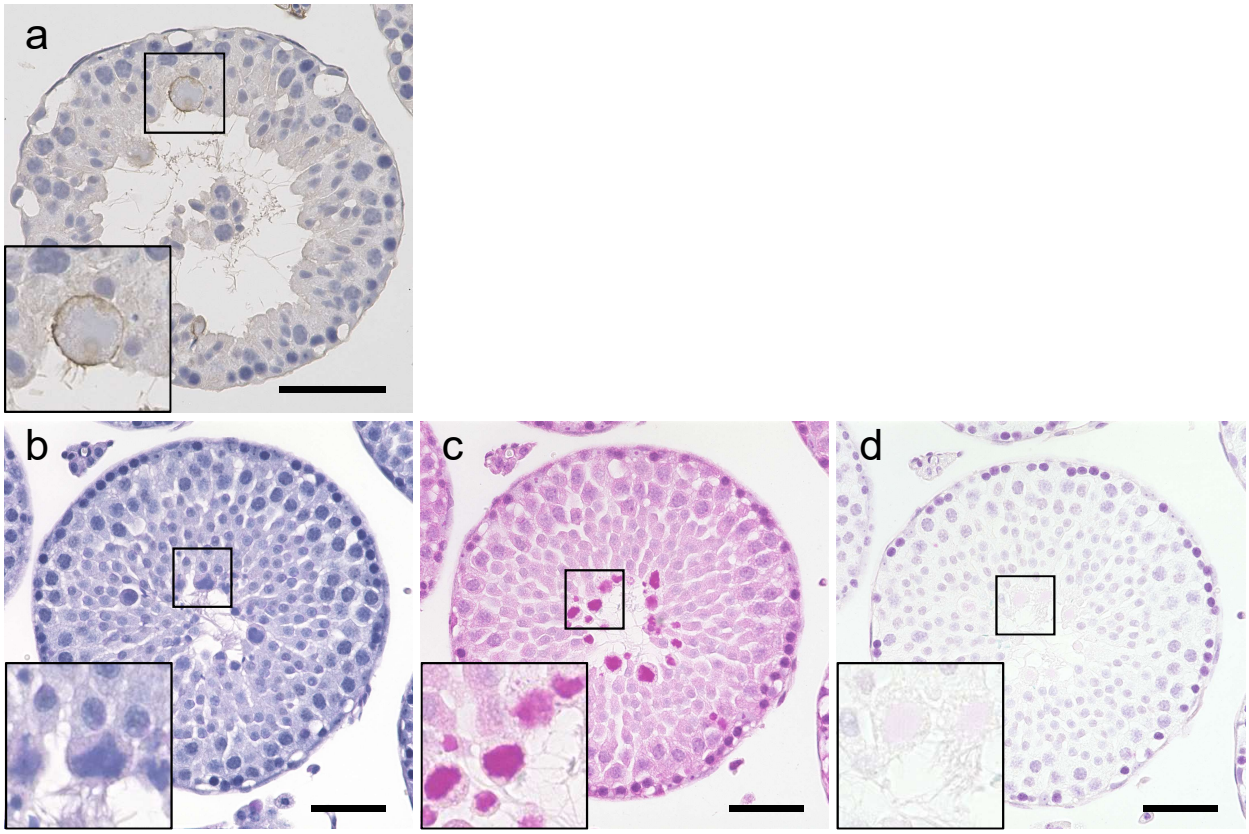

Supplemental Figure 2. Morphology of residual bodies in BXSB-*Yaa* seminiferous tubules.
(a) Immunohistochemistry for tACE in cross seminiferous tubules in BXSB-*Yaa* at 12 weeks of age. For antigen retrieval, deparaffinized sections were incubated in buffered citrate (pH 6.0) for 15 min at 110 ℃, and then the samples were soaked in methanol containing 0.3% H_2O_2 to block internal peroxidase activity. After blocked in 10% normal goat serum (SABPO(R) Kit, Nichirei, Tokyo, Japan) for 1 hour at room temperature, sections were incubated with antibody against mouse testicular isoform of angiotensin-converting enzyme (tACE, 1:50, MBL, Nagoya, Japan) at 4 ℃ overnight. After washing 3 times in phosphate buffered saline, sections were incubated with biotin-conjugated goat anti-mouse IgG antibody (SouthernBiotech, Alabama, USA) for 30 min at room temperature, washed again, and incubated with streptavidin-biotin complex (SABPO(R) Kit, Nichirei) for 30 min. The sections were then incubated with 3, 3'-diaminobenzidine tetrahydrochloride-H_2O_2 solution. Finally, the sections were counterstained with hematoxylin staining.
(b-d) Representative images of 12-week-old BXSB-*Yaa* seminiferous tubule stained with PAS-hematoxylin (b), methyl green-pyronin (c), and methyl green-pyronin with pre-treatment of RNase (d). To detect accumulated RNA in seminiferous tubules, deparaffinized sections were stained with methyl green-pyronin solution (Nacalai Tesque, Kyoto, Japan) for 10 min at room temperature, then washed with distilled water, and cleared with butanol (c). For further analysis, deparaffinized sections were treated with 0.01% RNase A (Nacalai Tesque, Kyoto, Japan) for 20 minutes at 37 ℃ before stained with methyl green-pyronin to confirm the existence of RNA (d). Bars = 50 μm. All sections were fixed in 4% paraformaldehyde.